# FGFR1 Is Required for the Development of the Auditory Sensory Epithelium

Ulla Pirvola,[1,2,4] Jukka Ylikoski,[1,2] Ras Trokovic,[1]
Jean M. Hébert,[3] Susan K. McConnell,[3]
and Juha Partanen[1]
[1]Institute of Biotechnology
[2]Department of Otolaryngology
00014 University of Helsinki
Finland
[3]Department of Biological Sciences
Stanford University
Stanford, California 94305

## Summary

The mammalian auditory sensory epithelium, the organ of Corti, comprises the hair cells and supporting cells that are pivotal for hearing function. The origin and development of their precursors are poorly understood. Here we show that loss-of-function mutations in mouse fibroblast growth factor receptor 1 (*Fgfr1*) cause a dose-dependent disruption of the organ of Corti. Full inactivation of *Fgfr1* in the inner ear epithelium by *Foxg1-Cre*-mediated deletion leads to an 85% reduction in the number of auditory hair cells. The primary cause appears to be reduced precursor cell proliferation in the early cochlear duct. Thus, during development, FGFR1 is required for the generation of the precursor pool, which gives rise to the auditory sensory epithelium. Our data also suggest that FGFR1 might have a distinct later role in intercellular signaling within the differentiating auditory sensory epithelium.

## Introduction

The mammalian auditory sensory epithelium, the organ of Corti (OC), is a cellular mosaic comprising the inner and outer hair cells (IHCs and OHCs) together with two types of supporting cells, the pillar and Deiter's cells. Retroviral marking studies have suggested that hair cells (HCs) and supporting cells of the avian hearing organ share common precursors (Fekete et al., 1998). Recent findings have shown that cell-cell communication within the presumptive OC has an instructive role in cell fate specification and differentiation. These processes critically depend on the proneural gene *Math1*, encoding a basic helix-loop-helix transcription factor, and on the components of the Notch signaling pathway (Bermingham et al., 1999; Eddison et al., 2000).

Before cellular differentiation, additional mechanisms must generate the precursor cell pool that gives rise to the OC. Thymidine incorporation experiments have shown that, in the mouse cochlea, the OC precursor cells enter terminal mitoses between E12 and E15 (Ruben, 1967). p27$^{Kip1}$, a cyclin-dependent kinase inhibitor, has been shown to promote the withdrawal of OC precursors from the cell cycle (Chen and Segil, 1999; Lowenheim et al., 1999). However, their origin, growth,
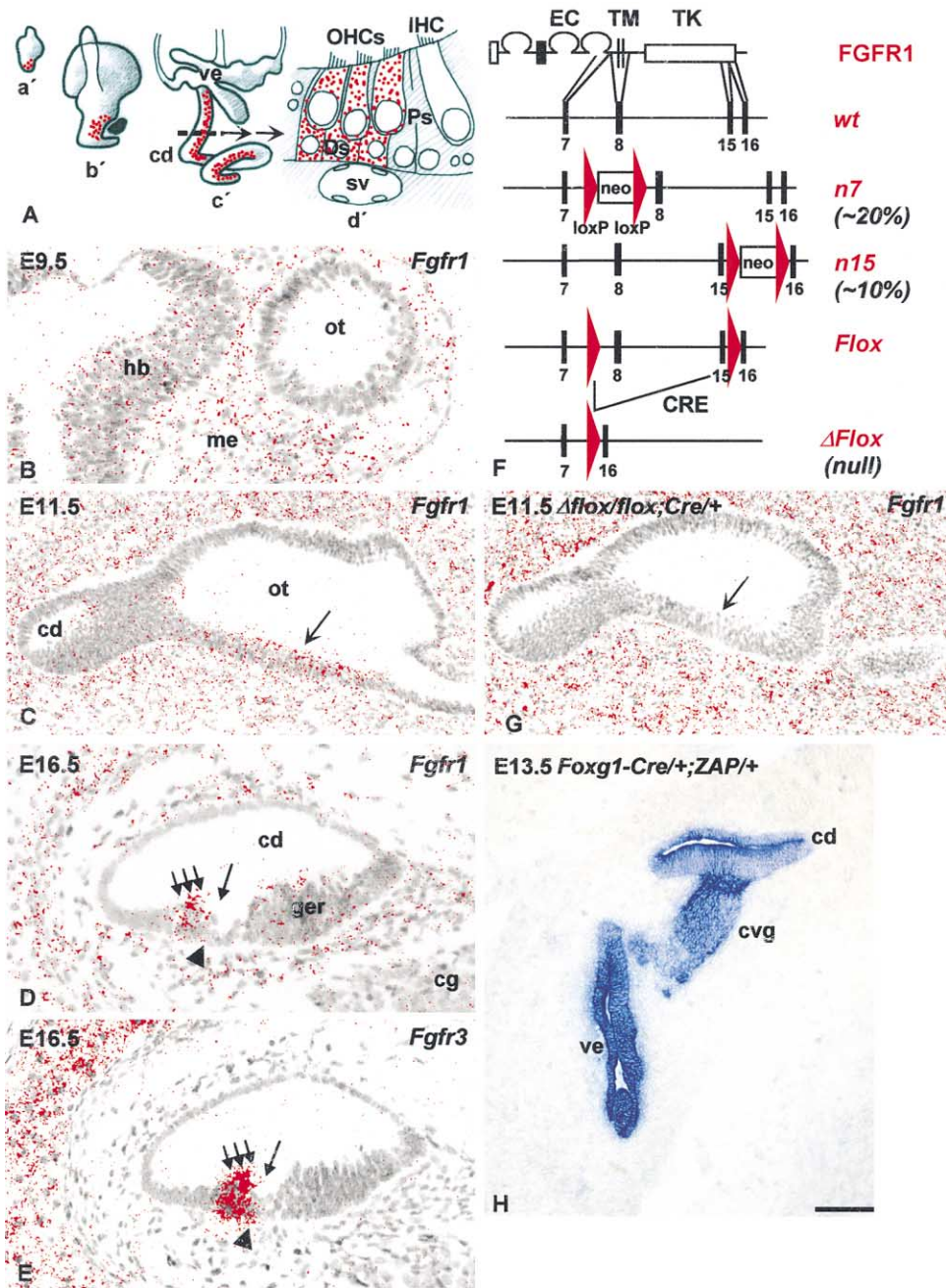
and the morphogenetic mechanisms, which direct the precursor cells to their correct position (i.e., the future OC), are poorly understood. No fate mapping studies of the cochlea exist, and thus the hypotheses on the origin of the different OC cell types are mostly based on histological analyses. Also the promitotic signals responsible for the expansion of the OC precursor cell pool are largely unknown. In addition to the developing cochlea, it is possible that cells possessing stem/precursor cell characteristics also exist in the mature hearing organ. Knowledge of the cell lineage and precursor cell regulation during development might be useful for the identification of these cells in the adult cochlea and perhaps even for their mitogenic reactivation and therapeutic HC regeneration.

Polypeptide growth factors, such as fibroblast growth factor 2 (FGF2) and epidermal growth factor, stimulate proliferation of neuronal precursor cells isolated from different regions of the developing central nervous system (for a review, see Gage, 2000). Several members of the FGF family are expressed in the developing inner ear, where FGF signaling has been implicated in induction and morphogenesis of the otic vesicle (Mansour et al., 1993; Ladher et al., 2000; Pirvola et al., 2000; Vendrell et al., 2000; Phillips et al., 2001) as well as cytodifferentiation within the OC (Colvin et al., 1996). We show here by partial loss-of-function and otic epithelium-specific null mutations that signaling by one of the FGF receptors, FGFR1, is essential for the formation of the OC. Our results suggest that auditory HCs and supporting cells are derived from a common precursor cell pool located in the ventromedial wall of cochlear duct and reveal an essential molecular mechanism that stimulates proliferation of these precursors of the OC.

## Results and Discussion

We have here analyzed the role of one of the FGF receptors, FGFR1, in the developing inner ear. We first studied *Fgfr1* mRNA expression by in situ hybridization (Figure 1). At embryonic day 9.5 (E9.5), *Fgfr1* was expressed at very low or undetectable levels in the otocyst (Figure 1B). *Fgfr1* expression was first detected at E10.5 in the ventromedial wall of the otocyst (Figure 1A). At E11.5, at the initial stages of cochlear duct outgrowth, *Fgfr1* expression extended from this ventromedial domain into the ventral wall of the nascent cochlear duct (Figure 1C). During the next few days, expression levels increased in the cochlear ventral wall, which comprises the primordial auditory sensory epithelium (Lim and Anniko, 1985). At E16.5, *Fgfr1* was detected in the medial, thickened region of the cochlear ventral wall, termed the greater epithelial ridge (GER), and together with *Fgfr3*, in differentiating OHCs and supporting cells of the more laterally located OC (Figures 1A, 1D, and 1E) (Peters et al., 1993). Concomitant to cellular maturation, *Fgfr1* expression was rapidly downregulated in the cochlear duct. In addition to the otic epithelium, the mesenchyme showed high numbers of *Fgfr1* transcripts throughout develop-

[4]Correspondence: ulla.pirvola@helsinki.fi

**Figure 1.** *Fgfr1* Expression in the Embryonic Inner Ear, Description of the Mutant *Fgfr1* Alleles Used in the Present Study, and the Pattern of *Foxg1-Cre*-Mediated Recombination

(A) The early otocyst at E10 (a′). The cochlear duct starts to grow out from the ventral wall of the otocyst between E11 and E12. The duct is extending at E13 (b′) and it spirals to contain 1¾ turns at E18.5 (c′). At late embryogenesis, the differentiating organ of Corti comprises IHCs and OHCs and two types of supporting cells, termed the Deiter's and pillar cells (d′). Red dots schematically depict *Fgfr1* expression in the otic epithelium.

(B) At E9.5, *Fgfr1* is expressed in the mesenchyme and hindbrain. No detectable expression is seen in the otocyst.
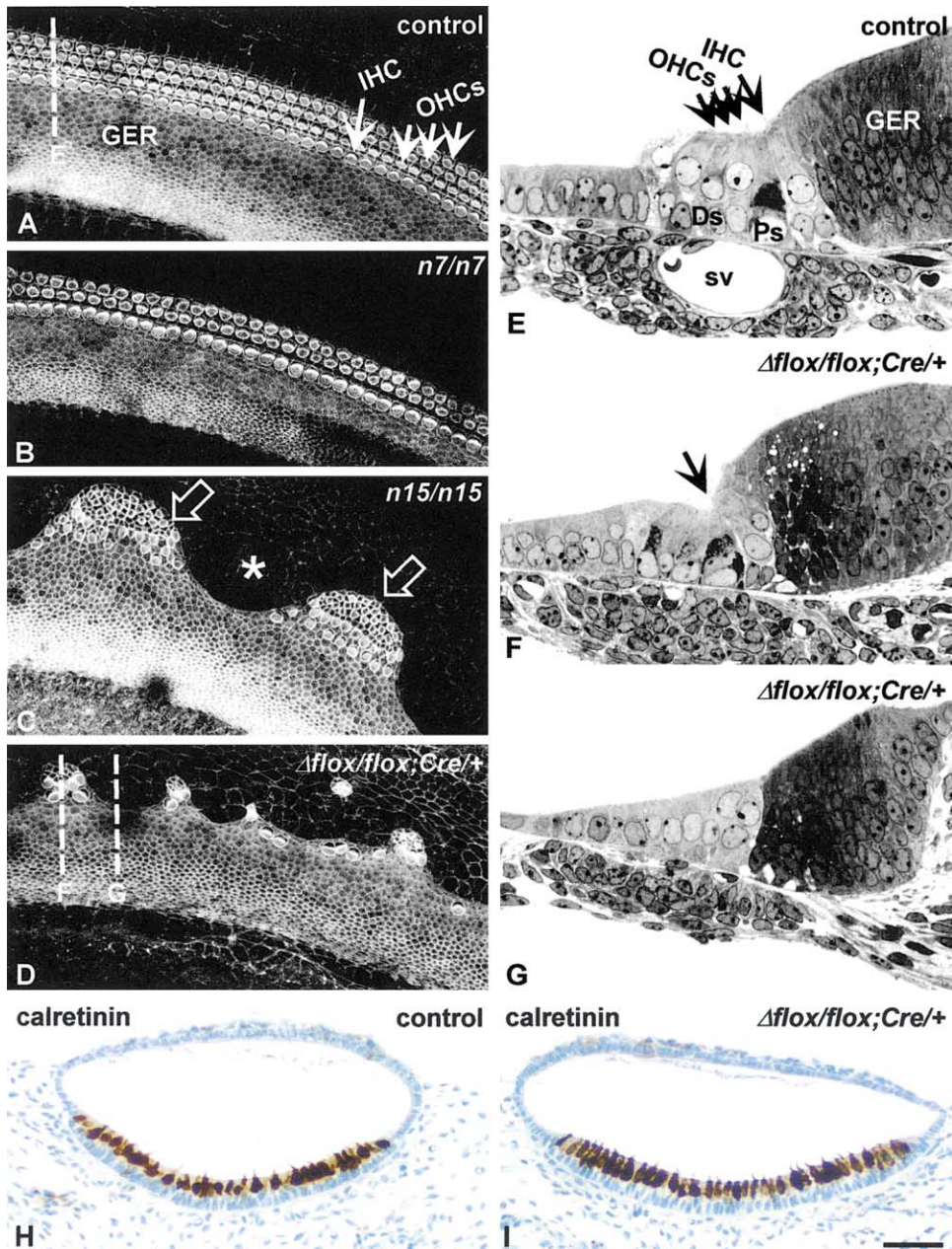
(C) At E11.5, in addition to the mesenchyme, *Fgfr1* is expressed in the ventromedial wall of the otocyst (arrow) and weakly in the ventral wall of the nascent cochlear duct.

(D and E) At E16.5, *Fgfr1* (D) and *Fgfr3* (E) are expressed in the differentiating organ of Corti (arrows) and in the mesenchyme. *Fgfr1* is also detected in the greater epithelial ridge. The short arrows mark the region of OHCs, long arrows the IHC. Pillar cells, which express *Fgfr3* but not *Fgfr1*, are marked by arrowheads.

(F) Structures of the FGFR1 protein and the wild-type *Fgfr1* locus are shown at the top. In *Fgfr1$^{n7}$* and *Fgfr1$^{n15YF}$* alleles, a neo cassette flanked by loxP sites is inserted into introns 7 and 15, respectively. *Fgfr1$^{flox}$* allele contains loxP sites in introns 7 and 15. Cre-mediated recombination results in excision of the DNA flanked by the loxP sites generating a null allele, *Fgfr1$^{\Delta flox}$*.

(G) Otocysts of the E11.5 *Fgfr1$^{\Delta flox/flox}$;Foxg1-Cre/+* mice do not show *Fgfr1* expression, as detected by a probe containing exon sequences between the loxP sites. The arrow marks the ventromedial wall. *Fgfr1* expression is maintained in the mesenchyme.

(H) Alkaline phosphatase staining of E13.5 *Foxg1-Cre/+;Z/AP/+* inner ears shows Cre-mediated recombination exclusively in the otic epithelium and the cochleovestibular ganglion. Abbreviations: ot, otocyst; cd, cochlear duct; me, mesenchyme; ve, vestibulum; sv, spiral vessel; IHC, inner hair cell, OHC, outer hair cell; Ps, pillar cells; Ds, Deiter's cells; ger, greater epithelial ridge; cg, cochlear ganglion; cvg, cochleovestibular ganglion. Scale bar in (H), 70 μm for (B), (D), and (E); 140 μm for (C) and (G); 200 μm for (H).

Figure 2. Disruption of the Organ of Corti, but Unaltered Vestibular Sensory Epithelium of FGFR1 Loss-Of-Function Mutant Mice

Phalloidin-stained surface specimens of the cochlea (A–D), semithin transverse sections through the organ of Corti (E–G), and calretinin-immunostained sections through the sacculus (H and I) at P0. (A) A control cochlea shows one continuous row of inner hair cell (IHCs) and three rows of outer hair cells (OHCs). The dotted line marks the orientation of sectioning in (E). (B–D) In $Fgfr1^{n7/n7}$ (B) and $Fgfr1^{n15YF/15YF}$ (C) hypomorphs and in $Fgfr1^{\Delta flox/flox};Foxg1-Cre/+$ mutants (D), the organ of Corti is disrupted in a dose-dependent fashion. The sensory patches of $Fgfr1^{n15YF/n15YF}$ and $Fgfr1^{\Delta flox/flox};Foxg1-Cre/+$ mutants are of variable size, and they frequently show doublet IHCs and an accumulation of disorientated IHCs at the edges. Open arrows in (C) point to the sensory patches, and the asterisk marks a gap between the patches. Dotted lines in (D) mark the orientation of sectioning in (F) and (G). (E–G) In contrast to normal cochleas (E), sections through the cochleas of $Fgfr1^{\Delta flox/flox};Foxg1-Cre/+$ mutants show IHCs and supporting cells without OHCs. Hair cells are identified by their cylindrical shape and by their stereocilia facing the lumen, and supporting cells by their dark cytoplasm (F). Several sections without any signs of differentiation of the organ of Corti are found in these cochleas (G). These sections represent the gaps between the sensory patches seen in surface specimens. (H and I) As detected by calretinin staining, the sacculus shows similar numbers of hair cells in control and $Fgfr1^{\Delta flox/flox};Foxg1-Cre/+$ mice. Abbreviations: IHC, inner hair cell; OHC, outer hair cell; GER, greater epithelial ridge; sv, spiral vessel; Ps, pillar cell; Ds, Deiter's cells. Scale bar in (I), 110 μm for (A)–(D); 25 μm for (E)–(G); 120 μm for (H) and (I).

ment (Figures 1B and 1C). Alternative splicing generates two *Fgfr1* isoforms, the *IIIb* and *IIIc* forms (Werner et al., 1992). By using isoform-specific probes, *Fgfr1* variants

were found to be coexpressed in the otic epithelium throughout development (data not shown). Taken together, *Fgfr1* is expressed at several stages of the devel-
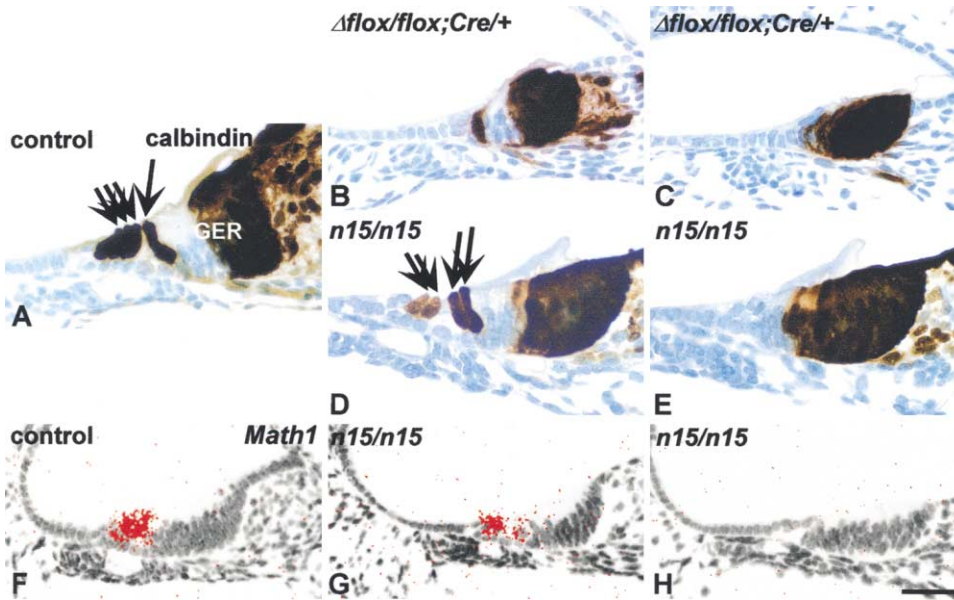
Figure 3. Cell Fate Specification and Differentiation in the Organ of Corti of FGFR1 Loss-Of-Function Mutant Mice

Calbindin immunohistochemistry and *Math1* in situ hybridization in transverse sections at E18.5.

(A) Calbindin staining reveals the normal pattern of one inner hair cell (IHC) (long arrow) and three outer hair cells (OHCs) (short arrows).

(B and C) $Fgfr1^{\Delta flox/flox};Foxg1-Cre/+$ mutants show only low numbers of calbindin-positive hair cells (IHCs) (B). Most sections are devoid of hair cells, and the greater epithelial ridge (GER) is thin (C).

(D and E) Sections through the cochleas of $Fgfr1^{n15YF/15YF}$ mice show variable numbers of OHCs and frequently doublet IHCs. Many hair cells appear shorter (D) than those in controls. Sections without any calbindin-stained hair cells are also found (E).

(F) *Math1* is expressed in hair cells of control cochleas.

(G and H) Cochleas of $Fgfr1^{n15YF/15YF}$ mutants comprise regions with *Math1*-expressing hair cells (G) and regions without any signs of hair cell specification (H). Scale bar in (H), 30 μm for (A)–(E); 50 μm for (F)–(H).

oping inner ear, especially in regions contributing to the formation of the OC.

To study the function of FGFR1 in the developing inner ear, we analyzed mice carrying loss-of-function mutations in the *Fgfr1* gene. *Fgfr1* null mutants die during gastrulation (Deng et al., 1994; Yamaguchi et al., 1994). Therefore, we first studied the cochlear phenotype of mice homozygous for the hypomorphic *Fgfr1* alleles, $Fgfr1^{n7}$ and $Fgfr1^{n15YF}$, which cause 80% and 90% reductions in the levels of full-length *Fgfr1* transcripts, respectively (Figure 1F) (Partanen et al., 1998). Both $Fgfr1^{n7/n7}$ and $Fgfr1^{n15YF/n15YF}$ hypomorphs die within 24 hr after birth. Whole-mount cochlear surface specimens were prepared at birth and stained with phalloidin, which reveals the apical, mechanosensory region of HCs as well as the apical borders of the supporting cells located between HCs. The normal pattern of one row of IHCs and three rows of OHCs that extends through the cochlear duct (Figure 2A) was disrupted in both hypomorphs. In the milder $Fgfr1^{n7/n7}$ mice, the third OHC row was missing throughout the length of the cochlear duct (Figure 2B). In the stronger $Fgfr1^{n15YF/n15YF}$ mice, similar perturbations were seen in the lower half of the cochleas. In contrast, the sensory epithelium of the upper half of their cochleas was arranged in patches (open arrows in Figure 2C) rather than as continuous rows as seen in controls. The gaps (asterisk in Figure 2C) between the patches showed no signs of differentiation of HCs or supporting cells. In contrast to these disturbances in cellular development within the OC, cochlear morpho-

genesis appeared largely normal in both hypomorphs. These data point to a specific role of *Fgfr1* in the generation of the cells of the auditory sensory epithelium.

To gain more insight into the quantitative requirements of *Fgfr1* in the otic epithelium, we completely inactivated *Fgfr1* in this compartment. We took advantage of a mouse line carrying a conditional *Fgfr1* allele, $Fgfr1^{flox}$ (Figure 1F), which can be inactivated by Cre recombinase, and of the *Foxg1-Cre* mouse line in which the Cre coding sequence is targeted to the *Foxg1* locus (Hébert and McConnell, 2000). *Foxg1* is expressed in the otic vesicle (Hébert and McConnell, 2000), and thus the *Foxg1-Cre* mice offered a possible means of regionally inactivating *Fgfr1* in the epithelium of the developing inner ear. We therefore generated mice carrying one conditional ($Fgfr1^{flox}$) and one null ($Fgfr1^{\Delta flox}$) allele of *Fgfr1* as well as a *Foxg1-Cre* allele (Figure 1F). To verify *Fgfr1* inactivation by the *Foxg1-Cre* allele, we analyzed spatiotemporal expression of *Fgfr1* in $Fgfr1^{\Delta flox/flox};Foxg1-Cre/+$ embryos using a probe specific for the region deleted by Cre-mediated recombination. As analyzed at E10.5, E11.5, E13.5, and E16.5, the otocyst, but not the surrounding mesenchyme, of the conditionally inactivated embryos was devoid of *Fgfr1* expression (Figure 1G). These results indicate that *Foxg1-Cre*-mediated recombination is restricted to the otocyst and that it occurs at the initial stages of *Fgfr1* expression. We further confirmed tissue specificity of Cre-mediated recombination by crossing *Foxg1-Cre* mice with *Z/AP* reporter mice, which express placental alkaline phosphatase upon re-
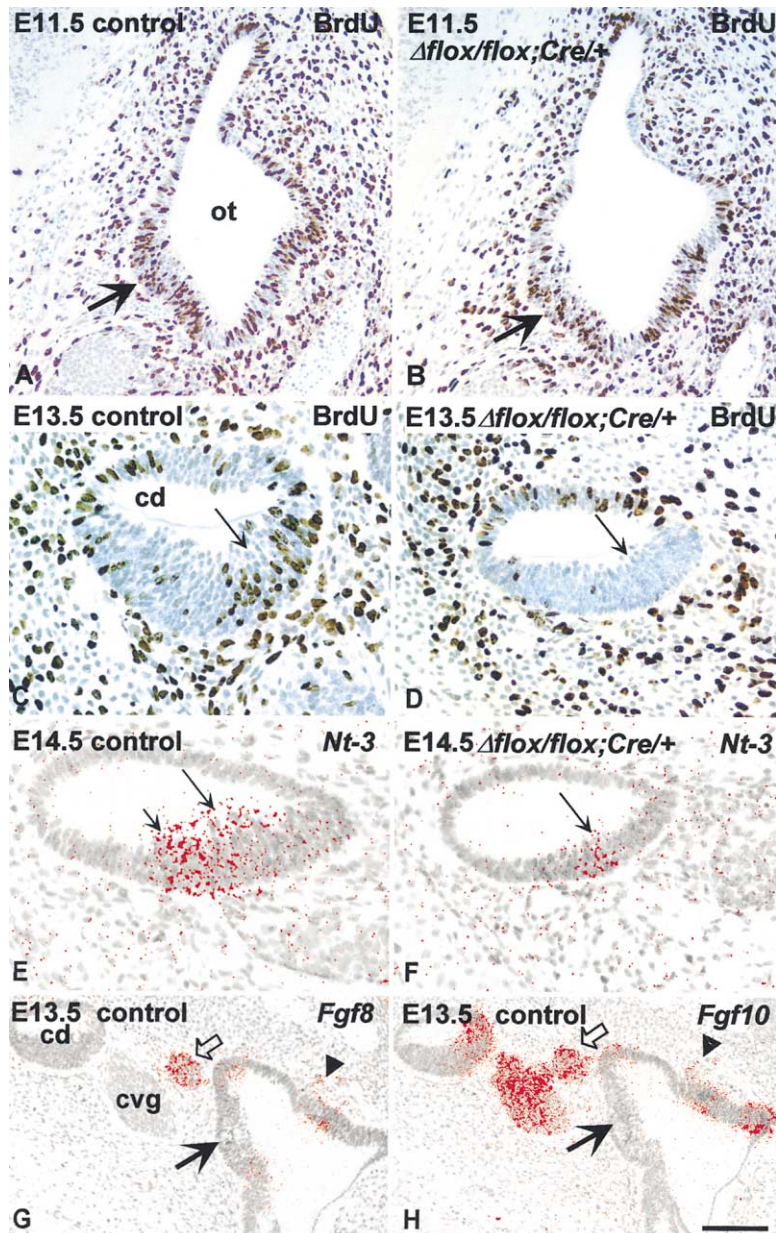
Figure 4. Impaired Production of Precursor Cells of the Organ of Corti in $Fgfr1^{\Delta flox/flox}$; $Foxg1$-$Cre$ Mice

Expression of $Fgfs$ at the stage when these precursors are generated.

(A and B) At E11.5, otocysts of both control (A) and mutant (B) embryos show intense BrdU labeling. Arrows mark the ventromedial wall.

(C and D) At E13.5, control mice show high numbers of BrdU-labeled cells in the greater epithelial ridge (arrow) (C). In the greater epithelial ridge (arrow) of mutants, numbers of BrdU-positive cells are markedly reduced (D).

(E and F) The cochlear duct of E14.5 control mice shows $Nt$-$3$ expression in the greater epithelial ridge (large arrow) and, more laterally, at the site of the presumptive organ of Corti (small arrow) (E). $Nt$-$3$ expression is markedly downregulated in the thin ventral wall of the cochlear duct of mutants (F).

(G) At E13.5, $Fgf8$ is expressed in the otic epithelium, including the junction of the outgrowing cochlear duct, and in delaminating neuroblasts (arrowhead and open arrow). The thick arrow marks the ventromedial wall of the otocyst.

(H) At E13.5, similar to $Fgf8$, $Fgf10$ is expressed in the otocyst, including the junction of the cochlear duct, and in delaminating neuroblasts (arrowhead and open arrow). Additionally, $Fgf10$ is found in the greater epithelial ridge and the cochleovestibular ganglion. Abbreviations: ot, otocyst; cd, cochlear duct; cvg, cochleovestibular ganglion. Scale bar in (H), 160 μm for (A) and (B); 70 μm for (C)–(F); 200 μm for (G) and (H).

combination (Lobe et al., 1999). Consistent with earlier data on E8.5–E11.5 embryos (Hébert and McConnell, 2000), the E13.5 double transgenic embryos ($Foxg1$-$Cre/+;Z/AP/+$) showed alkaline phosphatase staining in distinct, ectoderm-derived head structures, including the otocyst. Cre-mediated recombination was seen throughout the otic epithelium, including the nascent cochlear duct, and in the neurons of the cochleovestibular ganglion, which are derived from the otic epithelium (Figure 1H). The surrounding mesenchyme was negative. Thus, although $Fgfr1$ is expressed both in the epithelium and mesenchyme of the developing cochlea, our strategy provided a tool to study the role of $Fgfr1$ specifically in the epithelium, including HCs and supporting cells of the OC as well as their precursors.

Similar to the hypomorphs, $Fgfr1^{\Delta flox/flox}$;$Foxg1$-$Cre/+$ mutants died within 24 hr after birth. Around birth, phalloidin-stained cochlear surface specimens prepared from these mutants showed a severely disrupted OC. As compared to $Fgfr1^{n15YF/n15YF}$ hypomorphs, the sensory patches were reduced in size, and they mainly comprised IHCs and supporting cells (Figure 2D). Similar to the hypomorphs, the upper half of cochleas of $Fgfr1^{\Delta flox/flox}$;$Foxg1$-$Cre/+$ mice was more severely perturbed than the lower half. Only very low numbers of OHCs were formed, and these were located in the lower part of the cochleas. At postnatal day 0 (P0), the total number of differentiating HCs averaged 2212 ± 150 (n = 6 cochleas) in controls and 302 ± 54 (n = 9 cochleas) in $Fgfr1^{\Delta flox/flox}$;$Foxg1$-$Cre/+$ mutants (the apical region of the cochleas comprising immature HCs was not included in the counts). By counting differentiating OHCs only, these values were 1702 ± 112 (n = 6) and 37 ± 12 (n = 9), respectively. A comparable phenotype was

seen in *Fgfr1^flox/flox;Foxg1-Cre/+* mice (data not shown). Thus, *Fgfr1* regulates the numbers of HCs and supporting cells formed in a dose-dependent fashion, and interestingly, the requirement for *Fgfr1* varies along the length of the cochlear duct. In contrast to the OC, the morphology of the vestibular organs of the inner ear appeared normal in *Fgfr1^Δflox/flox;Foxg1-Cre/+* mice at birth. The presence of a normal complement of vestibular HCs was verified by using calretinin as a marker for these cells (Figures 2H and 2I).

We examined whether defects in cellular death, differentiation, fate specification, or proliferation account for the altered phenotype. In transverse sections at birth, the global morphology of the cochleas of *Fgfr1^Δflox/flox;Foxg1-Cre/+* mice was largely normal, except that frequently the cochleas were slightly shorter than in controls (data not shown). Between E13.5 and birth, morphological analysis and TUNEL staining (Figures 2E–2G, and data not shown) showed no differences in the extent of cell death in the ventral wall of the cochlear duct where precursors and, later, differentiating cells of the OC are located. Around birth, semithin sections through the control cochleas showed the characteristic pattern of one IHC, three OHCs, and the underlying supporting cells (Figure 2E). In contrast, in the sensory patches of *Fgfr1^Δflox/flox;Foxg1-Cre/+* mutants, IHCs were accompanied by supporting cells, but most sections were devoid of OHCs (Figure 2F). Sections through the gaps between the sensory patches showed no signs of cellular differentiation typical to the OC (Figure 2G).

By using molecular markers, we examined the possibility that precursors of the OC adopt their fates as HCs or supporting cells, but their morphological differentiation is blocked. Calbindin marks differentiating HCs. At birth, calbindin was expressed in HCs of control cochleas (Figure 3A). *Fgfr1^n15YF/n15YF* and especially *Fgfr1^Δflox/flox;Foxg1-Cre/+* mutants showed a marked reduction in the numbers of calbindin-positive HCs (Figures 3B–3E). *Math1* is involved in HC specification (Bermingham et al., 1999). As analyzed at E16.5 and at birth, *Math1* was expressed in HCs of control mice (Figure 3F). In the cochleas of *Fgfr1^n15YF/n15YF* mice, *Math1* transcripts were found in the sensory patches, but not in the intervening gap regions (Figures 3G and 3H). In these hypomorphs, similar regional distribution was observed for the Notch ligands *Delta1* (HCs; Eddison et al., 2000) and *Serrate1* (supporting cells; Eddison et al., 2000) (data not shown). In the cochleas of *Fgfr1^Δflox/flox;Foxg1-Cre/+* mice, the specification markers showed a very restricted expression (data not shown). These data indicate first, that there are no molecular signs of HC specification or differentiation in the gap regions and second, that the remaining HCs in the sensory patches undergo normal differentiation. Together with the fact that the altered phenotypes were evident already between E15.5 and E16.5 (data not shown), at the onset of cellular differentiation, these data suggest that *Fgfr1* mutations act on developmental events occurring before specification and differentiation processes.

To determine whether early patterning defects could explain the altered cochlear phenotype, we examined otocysts of *Fgfr1^Δflox/flox;Foxg1-Cre/+* mutants at E10.5
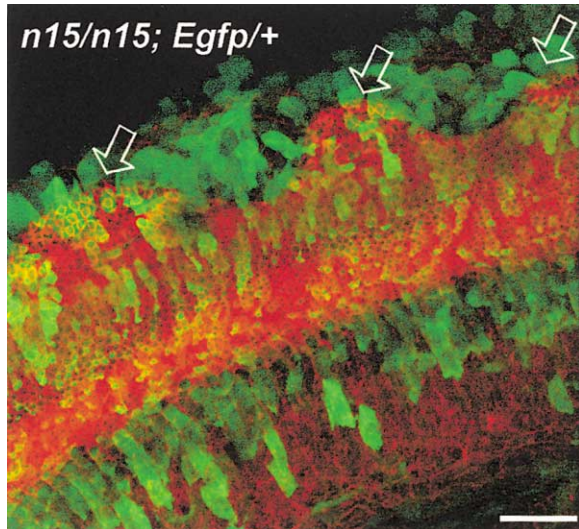


Figure 5. Clonal Analysis in the Cochleas of Hypomorphic *Fgfr1* Mutants

Whole mounts of E18.5 *Fgfr1^n15YF/n15YF;D4/XEgfp/+* embryos were double labeled with phalloidin (red) and an EGFP antibody (green). Cells of the sensory patches (open arrows) are not clonally related, as evidenced by heterogenous EGFP staining. Scale bar, 50 μm.

and E11.5. This was relevant since, as described above, *Fgfr1* is expressed at these stages in the ventromedial wall of the otocyst. We could not see differences between otocysts of mutants and controls in cellular proliferation (Figures 4A and 4B), cellular death, or in the expression of genes, such as *neurotrophin-3 (Nt-3)*, *Fgf10*, *Fgf8*, *Pax2*, *Gbx2*, *Notch1*, *Serrate1*, *Delta 1*, and *Lunatic Fringe*, which mark the different domains of the otic epithelium (data not shown). Additionally, at E12, no morphological differences were seen in the initiation of cochlear duct outgrowth from the otocyst. This stands in contrast to the role of *Fgfr2(IIIb)*, which is essential for the budding morphogenesis of the inner ear (Pirvola et al., 2000). As described above, the vestibular sensory epithelia of *Fgfr1^Δflox/flox;Foxg1-Cre/+* animals showed no abnormalities (Figures 2H and 2I). As the cochlear and part of the vestibular sensory epithelia are thought to derive from the same region of the otocyst, this result further supports our conclusion that patterning of the early otocyst is not altered in *Fgfr1* mutants.

The possibility still remained that the generation of the pool of precursor cells giving rise to the OC is affected by *Fgfr1* mutations. In the mouse, these precursors exit the cell cycle between E12 and E15 (Ruben, 1967). As assessed by bromodeoxyuridine (BrdU) incorporation, *Fgfr1^Δflox/flox;Foxg1-Cre/+* mice showed a reduction in proliferation rate in the ventral wall of the cochlear duct. Attenuation of proliferation was evident already at E12, but became very prominent between E13.5 and E15.5 (Figures 4C and 4D). Quantitative analysis performed between E13.5 and E14.5 revealed highly significant differences ($p < 0.005$) between mutants (7.7 ± 2.4 BrdU-labeled cells in the GER per section, n = 12 cochleas) and control littermates (57.4 ± 13.5, n = 12). At E14.5 and thereafter, impaired proliferation resulted in a thinner GER and a marked reduction in the level of *Nt-3*,
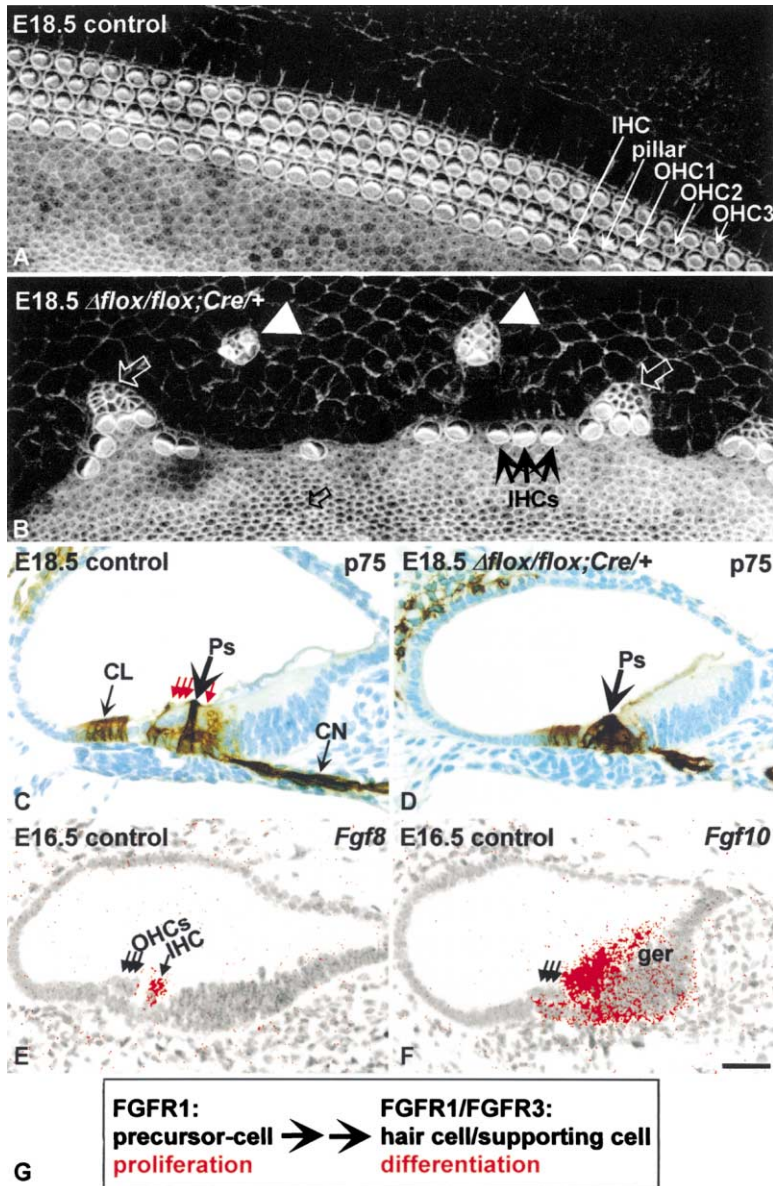
Figure 6. Altered Cytoarchitecture of the Organ of Corti of $Fgfr1^{\Delta flox/flox};Foxg1-Cre/+$ Mutant Mice at E18.5

Expression of *Fgfs* in the organ of Corti at E16.5.

(A and B) Phalloidin-stained surface specimens of the organ of Corti show the normal pattern of four hair cell rows and intervening apical processes of supporting cells (A). In mutants, this pattern is replaced by sensory patches (open arrows) with no or only a few outer hair cells (OHCs). In addition to the patches, small islands of sensory epithelium (arrowheads), invariably including at least a few hair cells, are found outside the normal area of the organ of Corti (B).

(C and D) As compared to controls (C), p75 labeling shows clusters of pillar cells (Ps) in the sensory patches of mutant mice (D). In addition to pillar cells, p75 is expressed in the cochlear nerve (CN) and Claudius cells (CL). Red arrows point to hair cells.

(E) In the differentiating organ of Corti, *Fgf8* is expressed exclusively in the inner hair cells (IHCs).

(F) At the same stage, *Fgf10* is found in the greater epithelial ridge (ger), especially in the region of IHCs.

(G) Proposed roles of FGFR1 during inner ear development. In the otocyst, FGFR1 stimulates proliferation of the precursors of the organ of Corti. During late embryogenesis, FGFR1—together with FGFR3—is suggested to promote cytodifferentiation within the organ of Corti. Scale bar in (F), 40 µm for (A) and (B); 60 µm for (C) and (D); 50 µm for (E) and (F).

which marks the presumptive inner ear sensory epithelia (Figures 4E and 4F) (Pirvola et al., 1992). Notably, no differences in proliferation rate between mutants and controls were seen in the dorsal, nonsensory wall of the cochlear duct (Figures 4C and 4D). Thus, our data indicate that FGFR1 signaling stimulates precursor cell proliferation specifically in the sensory compartment of the cochlea, and impaired proliferation is likely to account for the absence of large numbers of HCs and supporting cells, as seen in *Fgfr1* mutants at birth.

We next examined the nature and source of FGF ligands that might interact with FGFR1 to regulate the size of the progenitor pool of the OC. Of the several *Fgfs* analyzed between E11.5 and E14.5, *Fgf8* and *Fgf10* were found to be expressed in a spatiotemporal pattern, which appears relevant for our studies. *Fgf8* and *Fgf10* are expressed in the ventral part of the otocyst and in the delaminating cochleovestibular neuroblasts (Figures 4G and 4H) (Pirvola et al., 2000). Additionally, *Fgf10* was

found in the neurons of the cochleovestibular ganglion and, similar to *Fgfr1*, in the GER of the cochlear duct (Figure 4H). Available data on *neurogenin1* and *neurotrophin* knockout mice, in which the cochleovestibular ganglion is not formed or it degenerates soon after compaction, indicate that the neurons or migrating neuroblasts do not have a major impact on HC development (Fritzsch et al., 1997; Ma et al., 2000). Therefore, stimulation of proliferation of the OC's progenitors is likely to depend on interaction between FGFs and FGFR1 within the otic epithelium. Ligand binding properties of FGFRs are regulated by alternative splicing. As described above, *Fgfr1(IIIb)* and *Fgfr1(IIIc)* isoforms, differing in their extracellular region (Werner et al., 1992), are coexpressed in the otic epithelium. Interestingly, FGF10 has been reported to bind to FGFR1(IIIb), but not to FGFR1 (IIIc) (Igarashi et al., 1998; Lu et al., 1999). We therefore analyzed the inner ear phenotype of *Fgfr1(IIIb)* mutant mice, which survive until adulthood ($Fgfr1^{IIIBL/IIIBL}$) (Parta-

nen et al., 1998). Adult $Fgfr1^{IIIBL/IIIBL}$ mice showed normal cochlear morphology and hearing function as measured by auditory brainstem responses (six mutant and six control littermates analyzed; data not shown). Together, these data indicate that FGF10/FGFR1(IIIb) interaction alone is insufficient for the generation of the cochlear sensory epithelium and argue for the importance of FGFs acting through FGFR1(IIIc) to stimulate precursor cell proliferation.

As seen at birth, the reduced numbers of HCs and supporting cells found in $Fgfr1^{\Delta flox/flox};Foxg1-Cre/+$ and $Fgfr1^{n15YF/n15YF}$ mutants were arranged in patches rather than being distributed in a scattered manner. A possible explanation for the spatial clustering of these cells is that the cells in the same patch are derived from a common precursor cell. To test this hypothesis, we used a mouse line in which enhanced green fluorescent protein (EGFP) is integrated into the X chromosome ($D4/XEgfp$ transgenic mice; Hadjantonakis et al., 1998). Random X inactivation, which occurs between E5.5 and E8.5 in the mouse (Tan et al., 1993), yields mosaic females in which 50% of cells are EGFP positive. We then generated $Fgfr1^{n15YF/n15YF}$ hypomorphs that showed EGFP mosaicism ($Fgfr1^{n15YF/n15YF};D4/XEgfp/+$). If cells in a sensory patch are clonally related, the patches should be uniformly either EGFP positive or negative. Doublestaining with phalloidin and EGFP antibodies revealed that the sensory patches are heterogenous for EGFP expression (Figure 5). Thus, the patchy arrangement of the OC seems to be caused by mechanisms other than clonality, perhaps by preferential adhesion of the precursors of HCs and supporting cells with each other.

Of the different cell types of the OC, the numbers of OHCs were most severely affected in $Fgfr1$ mutants (Figures 6A and 6B). By using morphological criteria and p75 as a molecular marker (von Bartheld et al., 1991), clusters of pillar cells, one type of supporting cell of the OC, were seen in the sensory patches of $Fgfr1^{\Delta flox/flox};Foxg1-Cre/+$ mice at birth (Figures 2F and 6A–6D). These results suggest that the remaining precursors of the OC preferentially differentiate into IHCs and pillar cells. Thus, in addition to stimulating precursor cell proliferation in the nascent cochlear duct, FGFR1 may have a distinct later function in the differentiating OC to promote especially OHC development. In line with this suggestion, $Fgfr1$ expression was detected in the early-differentiating OHCs (Figures 1A and 1D). $Fgfr3$, but not $Fgfr1$, is expressed the pillar cells (Figures 1A, 1D, and 1E), these results being consistent with the phenotype of $Fgfr3$ knockout mice in which pillar cells fail to differentiate (Colvin et al., 1996). Thus, these two FGFRs might have at least to some extent complementary functions during the OC's differentiation. IHCs, which are the first cell type to start to differentiate in the OC, express $Fgf8$ throughout life (Figure 6E, and data not shown). In addition, $Fgf10$ (Figure 6F) and $Fgf3$ (data not shown) are expressed in the region of differentiating IHCs. Thus, we suggest that pioneering cells of the OC, the IHCs, stimulate differentiation of their later-emerging neighbors through FGF/FGFR signaling, in a similar fashion as receptor tyrosine kinase signaling has been shown to regulate development of the sense organs of $Drosophila$ (Freeman, 1997).

In conclusion, this work has elucidated an essential signaling pathway, which stimulates proliferation of precursor cells of the OC (Figure 6G). During development of several cell populations, including neurons of the forebrain and olfactory bulb, a cell lineage progression from stem cells to rapidly dividing progenitors and further to mature quiescent cells has been proposed (Martens et al., 2000; Doetsch et al., 2002). Our data suggest that actively proliferating OC precursors reside in the GER of the cochlear duct. They may represent transit-amplifying cells that proliferate rapidly and symmetrically and gradually move to their final destination, the OC proper. In this location, the precursors exit the cell cycle and local cues direct their differentiation into HCs or supporting cells. Interestingly, the FGF-responsive neural precursors of the embryonic forebrain are also thought to undergo a phase of rapid symmetric cellular divisions to increase their population size (Martens et al., 2000). Furthermore, FGF signaling through FGFR1 has been suggested to stimulate proliferation of neural precursor cells (Tropepe et al., 1999; Vaccarino et al., 1999). Thus, the cellular and molecular mechanisms regulating the precursor cell pools in the developing OC and central nervous system may be related.

Unlike in the bird's hearing organ, the adult mammalian cochlea is thought to lack regenerative capacity. Future studies are needed to investigate whether precursors, perhaps genuine stem cells, exist in the mature cochlea, similarly as recently shown in the retina (Tropepe et al., 2000) and whether the downregulation of FGFR1 contributes to their quiescence. The present results might help to design strategies for activation and/or expansion of the precursor cell pool that could give rise to new HCs, even in the adult hearing organ.

## Experimental Procedures

### Mutant Mice
The alleles $Fgfr1^{n7}$ and $Fgfr1^{n15YF}$ as well as the generation of the $Fgfr1^{IIIBL/IIIBL}$ mutant mice have been described by Partanen et al. (1998). The generation and characterization of the $Fgfr1^{flox}$ and $Fgfr1^{\Delta flox}$ alleles will be described in detail elsewhere. Briefly, the $Fgfr1^{flox}$ allele contains two loxP sites inserted into introns flanking the exons 8–15 of the $Fgfr1$ gene (Figure 1F). Mice homozygous for the $Fgfr1^{flox}$ allele are phenotypically normal. Cre-mediated recombination of the $Fgfr1^{flox}$ allele creates the $Fgfr1^{\Delta flox}$ allele. Mice heterozygous for this allele are normal, whereas homozygotes show a phenotype similar to $Fgfr1$ null mutants described earlier (Yamaguchi et al., 1994). The $Foxg1-Cre$ mice have been described by Hébert and McConnell (2000), and the $D4/XEgfp$ mice carrying a X-chromosomal $Egfp$ transgene by Hadjantonakis et al. (1998). All the analyses were done in outbred genetic background (ICR).

### Cochlear Whole Mounts
Cochlear ducts were dissected from E18.5 and P0 mice and fixed in 4% paraformaldehyde (PFA) in phosphate buffered saline (PBS) (pH 7.2) overnight at 4°C. The tectorial membrane was removed. Whole-mount specimens were incubated with rhodamine-phalloidin (Molecular Probes) and mounted in Vectashield (Vector Laboratories, Burlingame, CA) (n = 12 control cochleas, n = 20 $Fgfr1^{\Delta flox/flox};Foxg1-Cre/+$ cochleas, n = 20 $Fgfr1^{n15YF/n15YF}$ cochleas, n = 6 $Fgfr1^{n7/n7}$ cochleas). Cochleas of $Fgfr1^{n15YF/n15YF};D4/XEgfp/+$ mice (n = 12) were double labeled with rhodamine-phalloidin and a polyclonal rabbit EGFP antibody (Molecular Probes, Eugene, OR), followed by incubation with Alexa 488-coupled secondary antibody (Molecular Probes). Images were captured using a Zeiss Axiovert 100/135 epifluorescent microscope (Göttingen, Germany) connected to a Bio-Rad MRC-1024 confocal laser scanning system (Hemel Hemstead, UK).

## Histology

Embryos between E8.5 and E16.5 and inner ears dissected at E18.5 and P0 were fixed in PFA as described above. Paraffin-embedded sections were cut at 5 μm in transverse plane. Sections were incubated with the rabbit polyclonal calbindin and calretinin antibodies (Swant, Bellinzona, Switzerland) and the polyclonal p75 antibody (a kind gift from Dr. M. Chao). Detection was done by the peroxidase ABC kit (Vector Laboratories) and 3′3′diaminobenzidine. Sections were counterstained with methyl green.

Pregnant females were injected intraperitoneally with BrdU (Amersham-Pharmacia, Buckinghamshire, UK) and killed 2 hr after injection. PFA-fixed paraffin sections were denatured with 2 N HCl, trypsinized, and incubated with a mouse monoclonal BrdU antibody (Amersham-Pharmacia). Detection and counterstaining were done as above. BrdU-labeled cells were counted from the GER of E13.5 and E14.5 cochleas. Eight mutant and 8 control embryos (16 cochleas per group, 4 to 5 sections from each cochlea) were included in the analysis. Values presented are the mean ± SD. Significance was determined using Student's t test.

Paraffin sections were used for in situ hybridization with $^{35}$S-labeled riboprobes, using a procedure described by Wilkinson and Green (1990). Pan-*Fgfr1*, *Fgfr1(IIIb)*, *Fgfr1(IIIc)*, *Math1*, *Pax2*, *Gbx2*, *Notch1*, *Delta1*, *Serrate1*, *Lunatic Fringe*, *Nt-3*, *Fgf10*, and *Fgf8* probes were used. For the analysis of *Fgfr1* inactivation by Cre-mediated recombination, a probe containing exon sequences between the loxP sites was used. Three specimens or more of both mutants and controls at each stage were used for each antibody and probe. An Olympus Provis microscope (Tokyo, Japan) and a Photometrics SenSys CCD videocamera (Tucson, AZ) were used to obtain digitized images.

For alkaline phosphatase staining, E13.5 *Foxg1-Cre/+;Z/AP/+* (n = 4) and control (n = 2) embryos were fixed in 4% PFA for 3 hr and cut to 7 μm thick cryostat sections. They were incubated in PBS at 70°C for 30 min to inactivate endogenous phosphatases, followed by incubation with BM purple (Roche, Mannheim, Germany) for 4 hr at room temperature to detect alkaline phosphatase activity. Kaiser's Gelatine (Roche) was used for mounting. Control specimens did not show any staining.

Cochleas (n = 5 controls, n = 6 *Fgfr1$^{\Delta flox/flox}$;Foxg1-Cre/+*, n = 6 *Fgfr1$^{n15YF/n15YF}$*) were dissected at birth and fixed in 2.5% glutaraldehyde in 0.1 M phosphate buffer (pH 7.2) overnight at 4°C, postfixed in 1% osmium tetroxide, and embedded in Epon. One micron thick plastic sections were cut in transverse plane and stained with toluidine blue.

## Acknowledgments

## References

Bermingham, N.A., Hassan, B.A., Price, S.D., Vollrath, M.A., Ben-Arie, N., Eatock, R.A., Bellen, H.J., Lysakowski, A., and Zoghbi, H.Y. (1999). Math1: an essential gene for the generation of inner ear hair cells. Science *284*, 1837–1841.

Chen, P., and Segil, N. (1999). P27$^{Kip1}$ links cell proliferation to morphogenesis in the developing organ of Corti. Development *126*, 1581–1590.

Colvin, J.S., Bohne, B.A., Harding, G.W., McEwen, D.G., and Ornitz, D.M. (1996). Skeletal overgrowth and deafness in mice lacking fibroblast frowth factor receptor 3. Nat. Genet. *12*, 390–397.

Deng, C.X., Wynshaw-Boris, A., Shen, M.M., Daugherty, C., Ornitz, D.M., and Leder, P. (1994). Murine FGFR-1 is required for early postimplantation growth and axial organization. Genes Dev. *8*, 3045–3057.

Doetsch, F., Verdugo, J.M., Caille, I., Alvarez-Buylla, A., Chao, M.V., and Casaccia-Bonnefil, P. (2002). Lack of the cell-cycle inhibitor p27Kip1 results in selective increase of transit-amplifying cells for adult neurogenesis. J. Neurosci. *22*, 2255–2264.

Eddison, M., Le Roux, I., and Lewis, J. (2000). Notch signaling in the development of the inner ear: lessons from Drosophila. Proc. Natl. Acad. Sci. USA *97*, 11692–11699.

Fekete, D.M., Muthukumar, S., and Karagogeos, D. (1998). Hair cells and supporting cells share a common progenitor in the avian inner ear. J. Neurosci. *18*, 7811–7821.

Freeman, M. (1997). Cell determination strategies in the Drosophila eye. Development *124*, 261–270.

Fritzsch, B., Farinas, I., and Reichardt, L.F. (1997). Lack of neurotrophin 3 causes losses of both classes of spiral ganglion neurons in the cochlea in a region-specific fashion. J. Neurosci. *17*, 6213–6225.

Gage, F.H. (2000). Mammalian neural stem cells. Science *287*, 1433–1438.

Hadjantonakis, A.K., Gertsenstein, M., Ikawa, M., Okabe, M., and Nagy, A. (1998). Non-invasive sexing of preimplantation stage mammalian embryos. Nat. Genet. *19*, 220–222.

Hébert, J.M., and McConnell, S.K. (2000). Targeting of cre to the Foxg1 (BF-1) locus mediates loxP recombination in the telencephalon and other developing head structures. Dev. Biol. *222*, 296–306.

Igarashi, M., Finch, P.W., and Aaronson, S.A. (1998). Characterization of recombinant human fibroblast growth factor (FGF)-10 reveals functional similarities with keratinocyte growth factor (FGF-7). J. Biol. Chem. *273*, 13230–13235.

Ladher, R.K., Anakwe, K.U., Gurney, A.L., Schoenwolf, G.C., and Francis-West, P.H. (2000). Identification of synergistic signals initiating inner ear development. Science *290*, 1965–1967.

Lim, D.J., and Anniko, M. (1985). Developmental morphology of the mouse inner ear. A scanning electron microscopic observation. Acta Otolaryngol. Suppl. *422*, 1–69.

Lobe, C.G., Koop, K.E., Kreppner, W., Lomeli, H., Gertsenstein, M., and Nagy, A. (1999). Z/AP, a double reporter for cre-mediated recombination. Dev. Biol. *208*, 281–292.

Lowenheim, H., Furness, D.N., Kil, J., Zinn, C., Gultig, K., Fero, M.L., Frost, D., Gummer, A.W., Roberts, J.M., Rubel, E.W., et al. (1999). Gene disruption of p27(Kip1) allows cell proliferation in the postnatal and adult organ of Corti. Proc. Natl. Acad. Sci. USA *96*, 4084–4088.

Lu, W., Luo, Y., Kan, M., and McKeehan, W.L. (1999). Fibroblast growth factor-10. A second candidate stromal to epithelial cell andromedin in prostate. J. Biol. Chem. *274*, 12827–12834.

Ma, Q., Anderson, D.J., and Fritzsch, B. (2000). Neurogenin1 null mutant ears develop fewer, morphologically normal hair cells in smaller sensory epithelia devoid of innervation. J. Assoc. Res. Otolaryngol. *1*, 129–143.

Mansour, S.L., Goddard, J.M., and Capecchi, M.R. (1993). Mice homozygous for a targeted disruption of the proto-oncogene int-2 have developmental defects in the tail and inner ear. Development *117*, 13–28.

Martens, D.J., Tropepe, V., and van der Kooy, D. (2000). Separate proliferation kinetics of fibroblast growth factor-responsive and epidermal growth factor-responsive neural stem cells within the embryonic forebrain germinal zone. J. Neurosci. *20*, 1085–1095.

Partanen, J., Schwartz, L., and Rossant, J. (1998). Opposite phenotypes of hypomorphic and Y766 phosphorylation site mutations reveal a function for Fgfr1 in anteroposterior patterning of mouse embryos. Genes Dev. *12*, 2332–2344.

Peters, K., Ornitz, D., Werner, S., and Williams, L. (1993). Unique expression of the GHG receptor 3 gene during mouse organogenesis. Dev. Biol. *155*, 423–430.

Phillips, B.T., Bolding, K., and Riley, B.B. (2001). Zebrafish fgf3 and fgf8 encode redundant functions required for otic placode induction. Dev. Biol. *235*, 351–365.

Pirvola, U., Ylikoski, J., Palgi, J., Lehtonen, E., Arumae, U., and Saarma, M. (1992). Brain-derived neurotrophic factor and neurotrophin 3 mRNAs in the peripheral target fields of developing inner ear ganglia. Proc. Natl. Acad. Sci. USA *89*, 9915–9919.

Pirvola, U., Spencer-Dene, B., Qing-Qun, L., Kettunen, P., Thesleff, I., Fritzsch, B., Dickson, C., and Ylikoski, J. (2000). FGF/FGFR-2(IIIb) signaling is essential for inner ear morphogenesis. J. Neurosci. *20*, 6125–6134.

Ruben, R.J. (1967). Development of the inner ear of the mouse: a radioautographic study of terminal mitoses. Acta Otolaryngol. Suppl. *220*, 1–44.

Tan, S.S., Williams, E.A., and Tam, P.P. (1993). X-chromosome inactivation occurs at different times in different tissues of the postimplantation mouse embryo. Nat. Genet. *3*, 170–174.

Tropepe, V., Sibilia, M., Ciruna, B.G., Rossant, J., Wagner, E.W., and van der Kooy, D. (1999). Distinct neural stem cells proliferate in response to EGF and FGF in the developing mouse telencephalon. Dev. Biol. *208*, 166–188.

Tropepe, V., Coles, B.L., Chiasson, B.J., Horsford, D.J., Elia, A.J., McInnes, R.R., and van der Kooy, D. (2000). Retinal stem cells in the adult mammalian eye. Science *287*, 2032–2036.

Vaccarino, F.M., Schwartz, M.L., Raballo, R., Nilsen, J., Rhee, J., Zhou, M., Doetschman, T., Coffin, J.D., Wyland, J.J., and Hung, Y.T. (1999). Changes in cerebral cortex size are governed by fibroblast growth factor during embryogenesis. Nat. Neurosci. *2*, 246–253.

Vendrell, V., Carnicero, E., Giraldez, F., Alonso, M.T., and Schimmang, T. (2000). Induction of inner ear fate by FGF3. Development *127*, 2011–2019.

von Bartheld, C.S., Patterson, S.L., Heuer, J.G., Wheeler, E.F., Bothwell, M., and Rubel, E.W. (1991). Expression of nerve growth factor (NGF) receptors in the developing inner ear of chick and rat. Development *113*, 455–470.

Werner, S., Duan, D.S., de Vries, C., Peters, K.G., Johnson, D.E., and Williams, L.T. (1992). Differential splicing in the extracellular region of fibroblast growth factor receptor 1 generates receptor variants with different ligand-binding specificities. Mol. Cell. Biol. *12*, 82–88.

Wilkinson, D.G., and Green, J. (1990). *In situ* hybridization and the three-dimensional construction of serial sections. In Postimplantation Mammalian Embryos, Copp, A.J., and Cockroft, D.L., eds. (New York: Oxford University Press, IRL), pp. 155–171.

Yamaguchi, T.P., Harpal, K., Henkemeyer, M., and Rossant, J. (1994). Fgfr-1 is required for embryonic growth and mesodermal patterning during mouse gastrulation. Genes Dev. *8*, 3032–3044.